

## A Cephalosporin Prochelator Inhibits New Delhi Metallo- $\beta$ -Lactamase 1 without Removing Zinc

Abigail C. Jackson, Jacqueline M. Zaengle-Barone, Elena A. Puccio, and Katherine J. Franz

*ACS Infect. Dis.*, **Just Accepted Manuscript** • DOI: 10.1021/acsinfecdis.0c00083 • Publication Date (Web): 16 Apr 2020

Downloaded from [pubs.acs.org](https://pubs.acs.org) on April 17, 2020

### Just Accepted

“Just Accepted” manuscripts have been peer-reviewed and accepted for publication. They are posted online prior to technical editing, formatting for publication and author proofing. The American Chemical Society provides “Just Accepted” as a service to the research community to expedite the dissemination of scientific material as soon as possible after acceptance. “Just Accepted” manuscripts appear in full in PDF format accompanied by an HTML abstract. “Just Accepted” manuscripts have been fully peer reviewed, but should not be considered the official version of record. They are citable by the Digital Object Identifier (DOI®). “Just Accepted” is an optional service offered to authors. Therefore, the “Just Accepted” Web site may not include all articles that will be published in the journal. After a manuscript is technically edited and formatted, it will be removed from the “Just Accepted” Web site and published as an ASAP article. Note that technical editing may introduce minor changes to the manuscript text and/or graphics which could affect content, and all legal disclaimers and ethical guidelines that apply to the journal pertain. ACS cannot be held responsible for errors or consequences arising from the use of information contained in these “Just Accepted” manuscripts.

## A Cephalosporin Prochelator Inhibits New Delhi Metallo- $\beta$ -Lactamase 1 without Removing Zinc

Abigail C. Jackson, Jacqueline M. Zaengle-Barone, Elena A. Puccio, Katherine J. Franz\*

Department of Chemistry, Duke University, 124 Science Drive, Durham, North Carolina 27708, United States

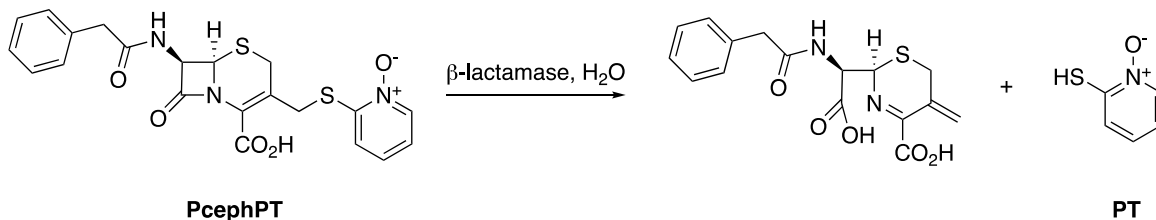
Antibacterial drug resistance is a rapidly growing clinical threat, partially due to expression of  $\beta$ -lactamase enzymes, which confer resistance to bacteria by hydrolyzing and inactivating  $\beta$ -lactam antibiotics. The increasing prevalence of metallo- $\beta$ -lactamases poses a unique challenge, as currently available  $\beta$ -lactamase inhibitors target the active site of serine  $\beta$ -lactamases but are ineffective against the zinc-containing active sites of metallo- $\beta$ -lactamases. There is an urgent need for metallo- $\beta$ -lactamase inhibitors and antibiotics that circumvent resistance mediated by metallo- $\beta$ -lactamases in order to extend the utility of existing  $\beta$ -lactam antibiotics for treating infection. Here we investigated the antibacterial chelator-releasing prodrug PcephPT (2-((((6*R*,7*R*)-2-carboxy-8-oxo-7-(2-phenylacetamido)-5-thia-1-azabicyclo[4.2.0]oct-2-en-3-yl)methyl)thio)pyridine 1-oxide) as an inhibitor of New Delhi metallo- $\beta$ -lactamase 1 (NDM-1). PcephPT is an experimental compound that we have previously shown inhibits growth of  $\beta$ -lactamase-expressing *E. coli* using a mechanism that is dependent on both copper availability and  $\beta$ -lactamase expression. Here, we found that PcephPT, in addition to being a copper-dependent antibacterial compound, inhibits hydrolysis activity of purified NDM-1 with an  $IC_{50}$  of 7.6  $\mu$ M without removing zinc from the active site and restores activity of the carbapenem antibiotic meropenem against NDM-1-producing *E. coli*. This work demonstrates that targeting a metal-binding pharmacophore to  $\beta$ -lactamase-producing bacteria is a promising strategy for inhibition of both bacterial growth and metallo- $\beta$ -lactamases.

1  
2  
3  
4  
5 Keywords:  $\beta$ -lactamase, resistance, prodrug, antibacterial, zinc, chelation  
6  
7  
8

9  
10 The spread of antibacterial drug resistance in pathogenic bacteria is a growing clinical  
11 threat. A common drug resistance mechanism exploited by bacteria is expression of  $\beta$ -lactamase  
12 enzymes that hydrolyze and inactivate a wide range of antibiotics in the  $\beta$ -lactam class, including  
13 penicillins, cephalosporins, and carbapenems.<sup>1</sup>  $\beta$ -lactamase inhibitors, such as clavulanic acid,  
14 sulbactam, and tazobactam, are often used in combination with  $\beta$ -lactam antibiotics to restore  
15 bactericidal efficacy. These inhibitors, however, target serine  $\beta$ -lactamases and are not effective  
16 against the emerging threat posed by metallo- $\beta$ -lactamases, which use catalytic zinc ions in their  
17 active sites to cleave the  $\beta$ -lactam ring.<sup>2-4</sup> There is an urgent need for potent inhibitors of metallo-  
18  $\beta$ -lactamases as well as antibiotics that can bypass metallo- $\beta$ -lactamase-mediated resistance, if  
19  $\beta$ -lactam antibiotics are to remain effective options for treatment of bacterial infection.  
20  
21  
22  
23  
24  
25  
26  
27  
28  
29

30 As part of our previous work on developing antibiotics that can overcome  $\beta$ -lactamase-  
31 mediated resistance, we reported the copper-dependent antibacterial activity of a prochelator we  
32 named PcephPT. PcephPT is a prodrug built on a cephalosporin core that is cleaved upon  
33 reaction with cephalosporinase and carbapenemase enzymes to release a metal chelating agent  
34 (**Scheme 1**).<sup>5</sup> The release of a leaving group at the 3' position of a cephalosporin after hydrolysis  
35 by a  $\beta$ -lactamase has been exploited for use in both antibacterial and diagnostic applications.<sup>6-12</sup>  
36 The leaving group of PcephPT is pyrithione (PT), a well-studied antimicrobial compound with a  
37 bidentate metal-chelating motif. PT interferes with metal homeostasis and can induce  
38 hyperaccumulation of metals, including copper.<sup>5, 13-16</sup> Copper has antibacterial effects when  
39 misregulated or present at high concentrations in bacteria.<sup>17-19</sup> We previously reported that  
40 PcephPT has antibacterial activity against  $\beta$ -lactamase-expressing *E. coli* strains and that this  
41 activity is dependent on both copper availability and  $\beta$ -lactamase expression.<sup>5</sup> PcephPT and  
42 related pyrithione-releasing cephalosporins have also been demonstrated to have potent  
43  
44  
45  
46  
47  
48  
49  
50  
51  
52  
53  
54  
55  
56  
57  
58  
59  
60

antimycobacterial activity against both replicating and non-replicating *Mycobacterium tuberculosis* strains that are resistant to other  $\beta$ -lactam antibiotics.<sup>20</sup>



**Scheme 1.** Mechanism of prochelator PcephPT.

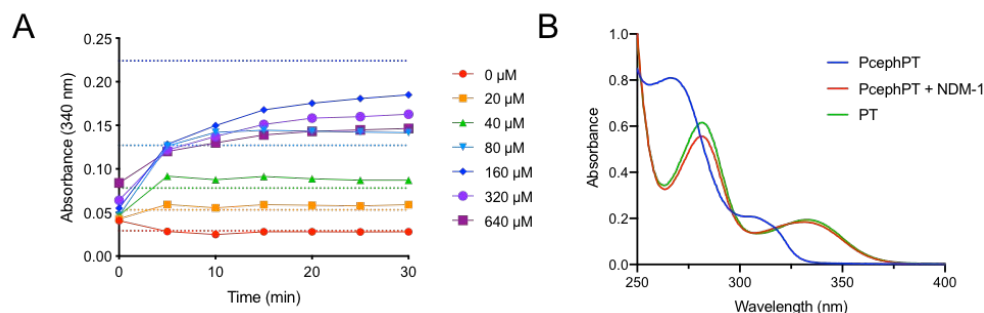
We hypothesized that PcephPT, in addition to being a promising antibacterial agent, may also inhibit metallo- $\beta$ -lactamases by releasing the chelator PT at the zinc-containing active sites of these enzymes. Many reported metallo- $\beta$ -lactamase inhibitors contain metal-binding pharmacophores that target the active site zinc ions; however, many of these agents may be problematic due to nonselective affinity for metals and metalloproteins, resulting in off-target effects.<sup>21</sup> Notably, PT and its copper complex have both been shown to inhibit NDM-1.<sup>22, 23</sup> The prochelator design of PcephPT is expected to have a significant mechanistic advantage over other metallo- $\beta$ -lactamase-inhibiting chelators because it delivers the inhibitor specifically to the resistance-causing enzyme, placing it in close proximity to the active site zinc ions and minimizing its interaction with the rest of the cellular metallome.

Here we explored the ability of PcephPT to inhibit New Delhi metallo- $\beta$ -lactamase 1 (NDM-1). NDM-1 is a class B1 di-zinc metallo- $\beta$ -lactamase that hydrolyzes nearly all  $\beta$ -lactam antibiotics, likely due to a flexible binding pocket that accommodates a wide variety of substrates.<sup>24, 25</sup> The gene encoding NDM-1 can easily be transferred between bacteria and is often found in pathogenic strains that also have other drug resistance genes.<sup>25, 26</sup> Currently there are no NDM-1 inhibitors approved by the US FDA. In the current work, we found that PcephPT has low- $\mu$ M inhibitory activity of NDM-1 and restores activity of a carbapenem antibiotic in carbapenem-

1  
2  
3 resistant *E. coli* strains expressing NDM-1. Our mechanistic studies revealed that neither  
4 PcephPT nor PT remove the zinc ions from the NDM-1 active site, unlike many known NDM-1-  
5 inhibiting chelators. Our results suggest that targeting chelators directly to  $\beta$ -lactamase-  
6 expressing bacteria is a promising strategy for targeted metallo- $\beta$ -lactamase inhibition in addition  
7 to metal-dependent antibacterial activity.  
8  
9  
10  
11  
12

## 13 Results and Discussion

14  
15  
16 **PT and PcephPT inhibit NDM-1.** The suitability of PcephPT as a substrate for NDM-1  
17 was validated spectroscopically by monitoring the characteristic absorbance of PT at 340 nm  
18 during reaction of PcephPT with purified NDM-1. PcephPT was turned over by 5 nM NDM-1  
19 efficiently at concentrations up to 160  $\mu$ M (**Figure 1A**). The final absorbance spectrum of  
20 PcephPT treated with NDM-1 at reaction completion matches that of PT, confirming that PT is  
21 indeed released during the reaction (**Figure 1B**).  
22  
23  
24  
25  
26  
27  
28  
29  
30



31  
32  
33  
34  
35  
36  
37  
38  
39  
40  
41  
42  
43 **Figure 1.** (A) Turnover of PcephPT by NDM-1. PT release from PcephPT was monitored on a plate  
44 reader at 340 nm upon treatment with 5 nM NDM-1 in HEPES buffer (50 mM, pH 7.2) at 37  $^{\circ}$ C. Dashed  
45 lines show the expected absorbance of PT (determined from a standard curve) if PcephPT at each  
46 concentration is turned over completely. (B) UV-Vis spectrum of 50  $\mu$ M PcephPT, 50  $\mu$ M PcephPT  
47 treated with 1 nM NDM-1 for 30 minutes at room temperature, and 50  $\mu$ M PT in HEPES (50 mM, pH  
48 7.2).  
49  
50  
51

52 The ability of PT and PcephPT to inhibit NDM-1 was tested in an *in vitro* assay using  
53 purified enzyme.<sup>27</sup> IC<sub>50</sub> values were determined by measuring turnover of the colorimetric  $\beta$ -  
54  
55  
56  
57  
58  
59  
60

1  
2  
3 lactamase substrate nitrocefin by 1 nM NDM-1 in the presence of each compound (**Table 1**,  
4 inhibition curves shown in **Figure S1**). For comparison, five other  $\beta$ -lactam antibiotics and three  
5 conventional chelators known to inhibit NDM-1 were also analyzed (**Figure 2**). PcephPT was  
6 found to inhibit NDM-1 under these conditions with an  $IC_{50}$  of 7.6  $\mu$ M, the lowest value among the  
7 antibiotics tested. Increasing its incubation time with NDM-1 did not affect its  $IC_{50}$  (**Figure S2**). In  
8 comparison, PT was a less effective inhibitor, with an  $IC_{50}$  of 17  $\mu$ M. Whereas the carbapenems  
9 imipenem and meropenem did not inhibit nitrocefin turnover (at the concentrations tested, up to  
10 320  $\mu$ M), the three cephalosporins tested were active, with  $IC_{50}$  values of 9.1, 16, and 36  $\mu$ M for  
11 cephalothin, ceftriaxone, and cephalexin, respectively. The hydrolysis products of these  
12 cephalosporins may be the culprit for this activity, as the isolated hydrolysis product of cephalothin  
13 has been previously reported to inhibit NDM-1, although with an  $IC_{50}$  higher than what we found  
14 here for cephalothin.<sup>28</sup> The discrepancy may be due to treatment with intact cephalothin, which  
15 releases the hydrolysis product directly to the active site. None of the  $\beta$ -lactams tested inhibited  
16 NDM-1 as well as PcephPT, suggesting that PcephPT has a structural or mechanistic advantage  
17 over most other cephalosporins leading to improved inhibition of NDM-1. We hypothesize that this  
18 improvement in inhibition could arise from the active inhibitor PT being released from PcephPT  
19 near the active site zinc ions, the intact or cleaved cephalosporin core of PcephPT contributing to  
20 inhibition, or a combination of these factors. PcephPT was less effective than the known NDM-1  
21 inhibitor dipicolinic acid (DPA) as well as two strong zinc-sequestering chelators, EDTA and TPEN  
22 (**Figure 2**).  
23  
24  
25  
26  
27  
28  
29  
30  
31  
32  
33  
34  
35  
36  
37  
38  
39  
40  
41  
42  
43  
44  
45  
46  
47  
48  
49  
50  
51  
52  
53  
54  
55  
56  
57  
58  
59  
60

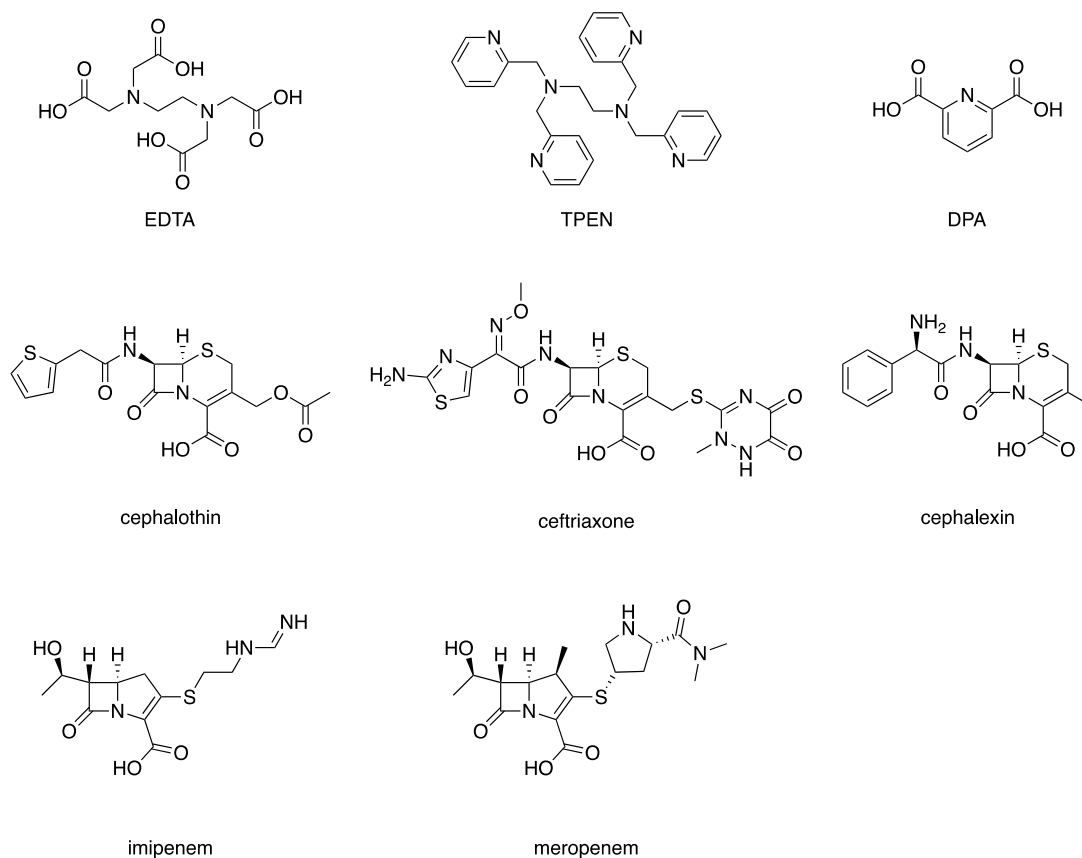


**Figure 2:** Structures of additional compounds tested for NDM-1 inhibitory activity. EDTA = ethylenediaminetetraacetic acid (used as the disodium salt in assays); TPEN = N,N,N',N'-tetrakis(2-pyridinylmethyl)-1,2-ethanediamine; DPA = dipicolinic acid.

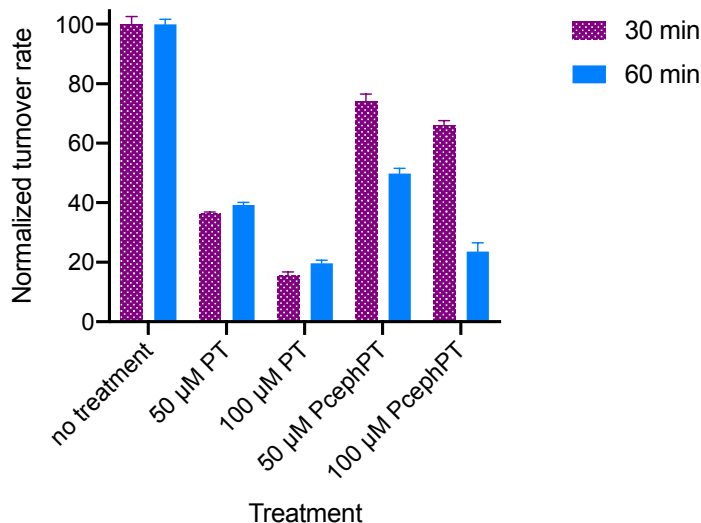
**Table 1.** IC<sub>50</sub> values for inhibition of NDM-1 by PcephPT, zinc chelators, known NDM-1 inhibitor dipicolinic acid (DPA), and β-lactam antibiotics, determined by measuring inhibition of nitrocefin turnover. 95% CI = 95% confidence interval of the IC<sub>50</sub>.

Compound	IC <sub>50</sub> (μM)	95% CI (μM)
PT	17	14–20
PcephPT	7.6	6.5–8.9
Cephalothin	9.1	6.5–13
Ceftriaxone	16	14–17

<b>Cephalexin</b>	36	25–49
<b>Imipenem</b>	>100	N/A
<b>Meropenem</b>	>100	N/A
<b>DPA</b>	1.8	0.58–2.8
<b>EDTA</b>	0.052	0.042–0.063
<b>TPEN</b>	0.088	0–0.10

**PT and PcephPT inhibit nitrocefin turnover in *E. coli* expressing NDM-1.** To determine efficacy of PT and PcephPT to inhibit NDM-1 activity in bacterial cells, nitrocefin turnover was tested in the cell lysate of an *E. coli* MG1655 strain expressing NDM-1. A culture was grown to an OD<sub>600</sub> of ~0.04 and treated with PT or PcephPT at either 50 μM or 100 μM for 30 or 60 minutes at room temperature, lysed by sonication, and immediately treated with nitrocefin. These concentrations and treatment lengths were chosen to minimize killing of the bacterial cells during treatment, while room temperature conditions were chosen to minimize growth. Preliminary experiments revealed that lysis of the bacterial culture was necessary to observe an increase in nitrocefin hydrolysis product, implying that NDM-1 is intracellular and nitrocefin does not penetrate the cell membrane sufficiently during the course of the assay. Even with PT or PcephPT treatment, lysis was necessary to observe nitrocefin turnover, indicating that PT and PcephPT do not cause lysis of the cells on their own. Turnover rates were observed for all treated conditions. At 100 μM, PT and PcephPT reduced nitrocefin turnover by more than 75% when treated for 60 minutes. (**Figure 3**). When cells were exposed to PcephPT for only 30 minutes, nitrocefin turnover was less inhibited, indicating that inhibition by PcephPT is time-dependent and a result of PcephPT reaching its target during the incubation period rather than inhibiting NDM-1 in the short period of time after sonication. These results indicate that both PT and PcephPT at least partially inhibit NDM-1 in the bacterial cellular environment. PT was able to

1  
2  
3 inhibit nitrocefin turnover to a greater extent than PcephPT, which may be due to a difference in  
4 membrane permeability between the two compounds or the relatively slow turnover of PcephPT,  
5  
6  
7 or both of these factors.  
8  
9



10  
11  
12  
13  
14  
15  
16  
17  
18  
19  
20  
21  
22  
23  
24  
25  
26  
27  
28  
29 **Figure 3:** Inhibition of nitrocefin turnover in NDM-1-expressing *E. coli* MG1655 treated with PT or  
30 PcephPT for 30 or 60 minutes.  
31  
32  
33  
34

35 **PcephPT restores activity of meropenem in NDM-1-expressing bacterial strains.** The  
36 compounds PT and PcephPT were tested in cultures of *E. coli* strains expressing NDM-1 to  
37 determine whether they can restore antibacterial activity of the carbapenem antibiotic  
38 meropenem, which has poor activity in NDM-1-expressing strains (MIC > 160 μM, **Table 2**). Two  
39 strains of *E. coli* were chosen for our study, the laboratory strain MG1655 and the pathogenic  
40 strain UTI89. As shown in our previous work, however, PT and PcephPT have antibacterial  
41 activity on their own.<sup>5</sup> In our strains expressing NDM-1, PT has an MIC of 20 μM in MG1655 or  
42 40 μM in UTI89, although growth is reduced at 20 μM. PcephPT did not completely inhibit growth  
43 in either strain at the highest concentration tested (160 μM), although growth was reduced by half  
44 at concentrations above 40 μM. Since NDM-1 inhibition on its own does not inhibit cell growth,  
45  
46  
47  
48  
49  
50  
51  
52  
53  
54  
55  
56  
57  
58  
59  
60

these prior results reveal inherent antibacterial activity independent of NDM-1 inhibition. With this activity in mind, we performed broth microdilution assays of meropenem with fixed concentrations of PT (10  $\mu$ M) or PcephPT (10 or 20  $\mu$ M). Under such conditions, PT and PcephPT would not inhibit growth, any growth inhibition could be attributed to recovery of meropenem efficacy.

At 10  $\mu$ M PT or PcephPT, meropenem activity was not restored in either strain. However, 20  $\mu$ M PcephPT reduced the meropenem MIC from >160  $\mu$ M to 10  $\mu$ M in both strains, which is consistent with inhibition of NDM-1 by PcephPT. The higher concentration of PT could not be used to measure meropenem activity recovery due to the antibacterial activity of PT at this concentration. The restoration of meropenem activity by PcephPT at a concentration of PcephPT so close to its  $IC_{50}$  (7.6  $\mu$ M) with purified enzyme is an impressive result, given that many reported NDM-1 inhibitors must be co-treated at much higher concentrations than their  $IC_{50}$ s in order to see a large decrease in carbapenem MIC in biological assays.<sup>29-34</sup> This relative potency suggests the delivery of PT directly to the active site of NDM-1 upon PcephPT turnover confers a distinct advantage. In susceptible strains, meropenem has an MIC lower than 10  $\mu$ M, so it is likely that PcephPT would inhibit NDM-1 more completely and further restore meropenem's activity if treated at concentrations higher than 20  $\mu$ M, but growth inhibition caused by meropenem would not be distinguishable from growth inhibition caused by PcephPT itself.

**Table 2.** Minimum inhibitory concentrations (MICs) of meropenem, NDM-1 inhibitors, and combinations. \*PcephPT caused at least a 50% reduction in growth at 40  $\mu$ M and higher but did not completely inhibit growth at any concentration tested. 160  $\mu$ M meropenem = 61  $\mu$ g/mL, 10  $\mu$ M meropenem = 3.8  $\mu$ g/mL, 20  $\mu$ M PT = 2.5  $\mu$ g/mL, 40  $\mu$ M PT = 5.1  $\mu$ g/mL, 20  $\mu$ M PcephPT = 9.1  $\mu$ g/mL, 160  $\mu$ M PcephPT = 73  $\mu$ g/mL.

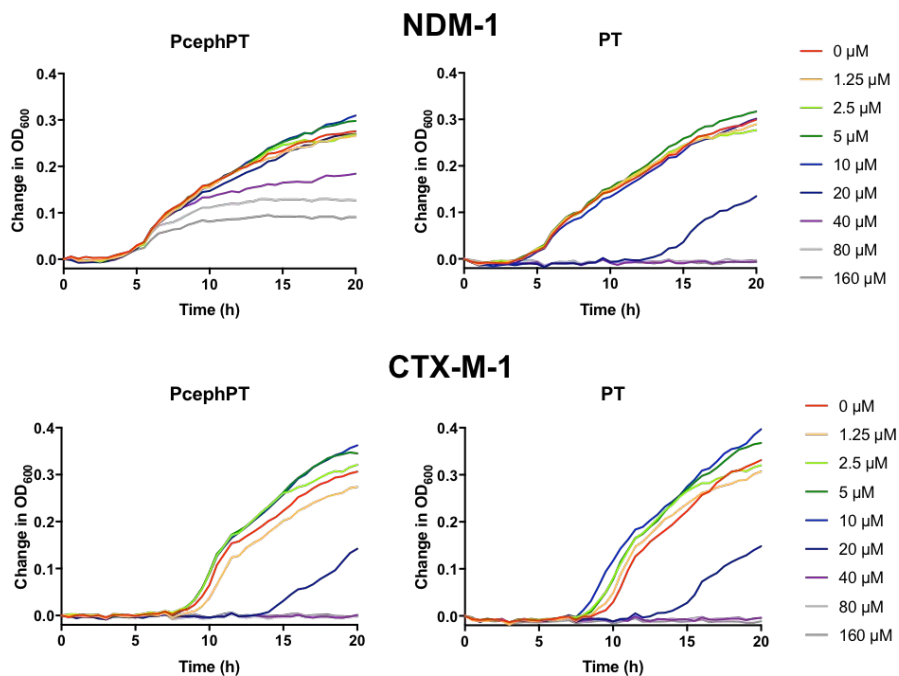
Compound	MG1655 MIC ( $\mu$ M)	UT189 MIC ( $\mu$ M)
Meropenem	>160	>160

PT	20	40
PcephPT	>160*	>160*
Meropenem + 10 $\mu$ M PT	160	160
Meropenem + 10 $\mu$ M PcephPT	160	160
Meropenem + 20 $\mu$ M PcephPT	10	10
Meropenem + 20 $\mu$ M cephalothin	>160	>160
Meropenem + 20 $\mu$ M ceftriaxone	>160	>160

**Growth inhibition by PcephPT is delayed in an NDM-1-expressing strain compared to a serine  $\beta$ -lactamase strain.** As noted previously, PcephPT reduces growth significantly at concentrations of 40  $\mu$ M and higher, but does not completely inhibit growth, even after 20 h at concentrations up to 160  $\mu$ M. To get a clearer picture of how these compounds influence growth pattern, antibacterial susceptibility assays were repeated by recording OD<sub>600</sub> measurements every 30 minutes over the course of the 20-hour incubation (**Figure 4**) for *E. coli* MG1655 strains expressing either NDM-1 or the serine  $\beta$ -lactamase CTX-M-1 for comparison. The growth of both strains was fully inhibited by concentrations of PT 20  $\mu$ M and higher, with delayed growth at 10  $\mu$ M PT. This growth response is consistent with bacteriostatic activity, where growth is inhibited without killing cells at concentrations near the MIC, allowing regrowth at later timepoints.<sup>35</sup> As we found previously, PT is bacteriostatic in the absence of supplemental copper.<sup>5</sup>

In the CTX-M-1-expressing strain, PcephPT caused a growth pattern identical to that caused by PT (**Figure 4**). This result was expected, since PcephPT releases PT quickly in this strain<sup>5</sup> and therefore it is expected to behave similarly to PT alone. However, a very different growth pattern was observed for NDM-1-expressing cells treated with PcephPT, with growth in all conditions initially followed by a delayed onset of growth inhibition at concentrations of 40  $\mu$ M and higher between five and eight hours of growth. This result is consistent with slow NDM-1-activated

1  
2  
3 release of PT from PcephPT in this strain, presumably due to product inhibition. This notion is  
4 supported by our previously published data demonstrating that the NDM-1-expressing strain  
5 shows slower turnover of PcephPT than strains expressing broad-spectrum serine- $\beta$ -  
6 lactamases.<sup>5</sup> Addition of copper made no significant difference in the growth pattern of PcephPT  
7 in the NDM-1 strain (**Figure S3**).



36  
37 **Figure 4.** Comparison of time-dependent growth curves of *E. coli* MG1655 strains expressing the  
38 metallo- $\beta$ -lactamase NDM-1 vs. the serine  $\beta$ -lactamase CTX-M-1 in the presence of varying  
39 concentrations of PcephPT and PT, illustrating the delayed antibacterial activity of PcephPT in the  
40 NDM-1-expressing strain. Growth in Mueller Hinton media at 37 °C was assessed by measuring OD<sub>600</sub>  
41 every 30 minutes.

42  
43  
44  
45  
46  
47  
48  
49 **The mode of inhibition is not metal removal from the NDM-1 active site.** The  
50 mechanism by which a compound inhibits NDM-1 has implications for its selectivity and is  
51 important to determine when developing inhibitors.<sup>21</sup> Two common mechanisms of NDM-1  
52 inhibition are removal of zinc from the active site (zinc stripping) and binding of an inhibitor within  
53  
54  
55  
56  
57  
58  
59  
60

1  
2  
3 the active site (ternary complex formation).<sup>21</sup> Each strategy has its challenges; for example, high-  
4 affinity metal chelators that operate via zinc stripping can interact with metalloproteins  
5 nonspecifically and cause other off-target effects, while ternary complex formers may not be  
6 effective against the broad spectrum of metallo- $\beta$ -lactamases.<sup>21</sup> The ability of NDM enzymes to  
7 evolve, including by developing tighter zinc binding sites under the pressure of zinc deprivation,<sup>36</sup>  
8 poses additional challenges associated with development of resistance, which may be impacted  
9 by the mechanism of inhibition.  
10  
11  
12  
13  
14  
15  
16  
17

18 To evaluate the mechanism of NDM-1 inhibition by PT and PcephPT, we used an  
19 equilibrium dialysis experiment to separate enzyme-bound inhibitors from those free in solution,  
20 including inhibitors bound to zinc ions that have been removed from the active site. Briefly, purified  
21 holo-NDM-1 enzyme was incubated with 40  $\mu$ M (four equivalents) or 160  $\mu$ M (sixteen equivalents)  
22 EDTA, PT, or PcephPT and dialyzed against buffer to separate small molecule species. Using  
23 methods based on previously published procedures,<sup>37</sup> the protein fraction was then denatured  
24 and the concentration of protein and zinc quantitated to determine the zinc content per NDM-1  
25 molecule (**Figure 5**).  
26  
27  
28  
29  
30  
31  
32  
33

34 Using this method, untreated NDM-1 was determined to contain 1.6 zinc atoms on  
35 average per molecule after dialysis. NDM-1 is capable of binding two zinc atoms, although one  
36 binds more strongly than the other,<sup>37</sup> which may explain the partial loss of zinc during dialysis.  
37 EDTA, a known metal-stripping agent, removed 85% of the zinc from NDM-1 when treated at 40  
38  $\mu$ M (four equivalents), while 160  $\mu$ M removed zinc completely. Treatment with PT and PcephPT,  
39 however, did not lead to loss of zinc from the active site when treated at either 40  $\mu$ M or 160  $\mu$ M.  
40 These data suggest that, at these concentrations, these inhibitors do not use the mechanism of  
41 zinc removal and are likely to form a ternary complex in the active site of NDM-1. Absorbance  
42 peaks corresponding to PT were not observed in the spectra of the dialyzed NDM-1 samples after  
43 treatment with PcephPT or PT; however, such peaks are not expected to have a large enough  
44 absorbance at the concentrations used to be visible among the other signals present. The  
45  
46  
47  
48  
49  
50  
51  
52  
53  
54  
55  
56  
57  
58  
59  
60

potential stable binding of PT to the active site without removal of zinc, in combination with the specific targeting provided by the  $\beta$ -lactamase-targeted core, makes prochelators like PcephPT very promising for use as NDM-1 inhibitors.

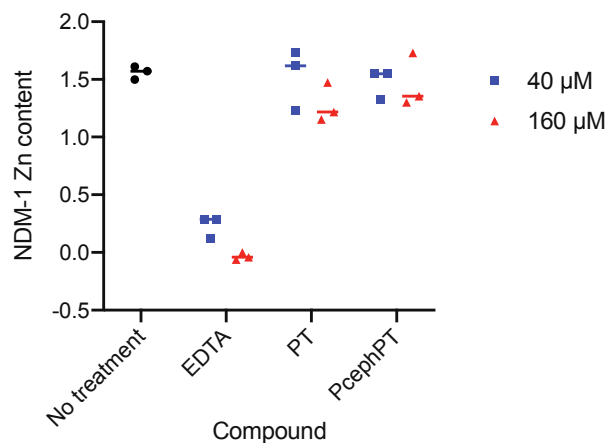
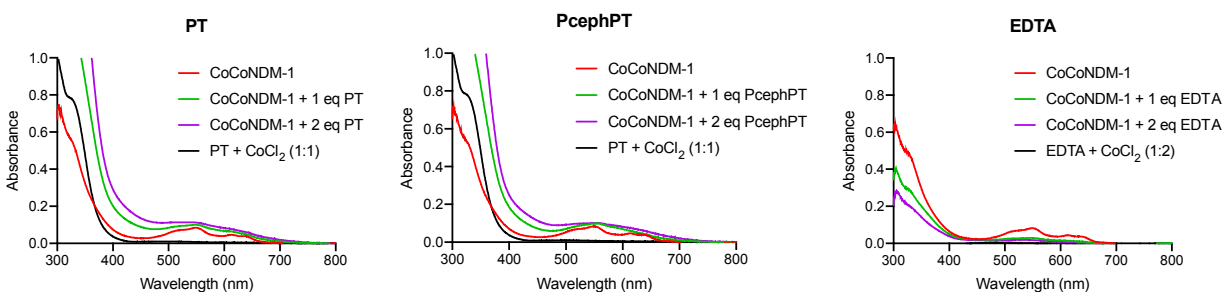


**Figure 5.** Zinc content of NDM-1 after treatment with compounds followed by equilibrium dialysis. Protein concentration was determined using  $A_{280}$  and zinc concentration was determined using the colorimetric chelator 4-(2-pyridylazo)resorcinol (PAR).

**UV-Visible spectra of CoCo-NDM-1 treated with PcephPT and PT support ternary complex formation.** Spectroscopy of cobalt(II)-substituted NDM-1 has often been used as a method to study interactions of inhibitors and substrates with the active site of NDM-1.<sup>21, 34, 37-40</sup> The two main features of the CoCo-NDM-1 spectrum that have been characterized previously are a strong peak at 330 nm corresponding to a Cys-Co(II) ligand-metal charge transfer band, and several smaller peaks in the 500–650 nm region corresponding to ligand field bands from the pseudotetrahedral Co(II) sites.<sup>39</sup> Addition of compounds that remove metal from the NDM-1 active site result in reduction of these absorbance features, while treatment with compounds that form a ternary complex may result in either changes in the shape or intensity of the peaks or an unchanged spectrum. Addition of PT or PcephPT to Co-substituted NDM-1 caused an increase in absorbance in the 500–650 nm region and smoothing of these peaks, as well as a large

1  
2  
3 increase in absorbance in the 300–400 nm region (**Figures 6** and **S4**). The increase in the charge  
4 transfer band below 400 nm in our spectrum would be consistent with an additional sulfur ligand  
5 bound to an active site cobalt, while the changes in the 500–600 nm region indicate other changes  
6 in the coordination environment. These results are consistent with the equilibrium dialysis data in  
7 supporting a mechanism involving ternary complex formation for PT binding to the active site  
8 metal ions of NDM-1. In comparison, EDTA, a known metal-stripping inhibitor, caused significant  
9 decreases in both regions of the spectrum.  
10  
11  
12  
13  
14  
15  
16  
17  
18  
19  
20



21  
22  
23  
24  
25  
26  
27  
28  
29  
30  
31 **Figure 6:** UV-Vis spectra of CoCo-NDM-1 (300  $\mu\text{M}$ ) treated with one or two equivalents of PT,  
32 PcephPT, or EDTA, compared to the spectra of 300  $\mu\text{M}$  PT or EDTA in the presence of excess  $\text{CoCl}_2$ .  
33 Control spectra of apo-NDM-1 (which is subtracted from all NDM-1 spectra here) and expansions of  
34 the 500–700 nm peaks are shown in **Figure S4**.  
35  
36  
37  
38  
39  
40

41 According to our equilibrium dialysis and UV-Vis experiments, PT and PcephPT do not  
42 remove zinc from the NDM-1 active site, suggesting that, if PT is binding to the zinc, it cannot  
43 bind strongly enough to compete with active site residues to remove zinc. A competitive inhibition  
44 mode may therefore be consistent with this result, since PT may be competing with substrate  
45 binding at the active site zinc. We examined the kinetics of nitrocefin turnover in the presence of  
46 our inhibitors and found that the kinetics of NDM-1 inhibition by PT or PcephPT do not fit well with  
47 any of the classical inhibition modes (competitive, uncompetitive, or noncompetitive). We could  
48 not confidently determine the trend in  $K_M$  values due to poor fitting with the low-concentration part  
49  
50  
51  
52  
53  
54  
55  
56  
57  
58  
59  
60

1  
2  
3 of the Michaelis-Menton curves, potentially resulting from low sensitivity in our assay at these  
4 concentrations. However, a clear decrease in  $V_{\max}$  observed with increasing inhibitor  
5 concentration (**Figure S5**) indicates that increasing substrate cannot recover NDM-1 activity,  
6 illustrating that the inhibition mode is not competitive.  
7  
8  
9  
10

## 11 12 13 **Conclusions**

14  
15 Here we have demonstrated that an antibacterial prochelator, PcephPT, inhibits the  
16 hydrolysis activity of the clinically significant metallo- $\beta$ -lactamase NDM-1. PT, the molecule  
17 released from PcephPT, is a bidentate metal-binding molecule that is known to complex a variety  
18 of metal ions, notably in this context the biologically relevant ions of zinc, copper and iron. Its lack  
19 of metal selectivity means that it potentially acts on multiple metal-dependent processes to  
20 influence cellular metallomes and inhibit microbial growth. Here we have expanded the utility of  
21 PT to include targeted NDM-1 inhibition when released from a prodrug. Enzymatic inhibition  
22 assays demonstrated an  $IC_{50}$  of 7.6  $\mu$ M for PcephPT, indicating that it is more potent than the  
23 chelator PT alone and comparable in efficacy to other reported NDM-1 inhibitors. PcephPT is able  
24 to restore antibacterial activity of meropenem, a carbapenem antibiotic that is readily hydrolyzed  
25 by NDM-1, and inhibit turnover of an NDM-1 colorimetric substrate in bacterial culture.  
26 Experiments exploring the kinetics of bacterial growth in the presence of PcephPT provide support  
27 for the dual mechanism involving both NDM-1 enzyme inhibition and PT-mediated growth  
28 inhibition. Equilibrium dialysis and quantification of zinc in PcephPT-treated NDM-1 indicates that  
29 zinc removal from the NDM-1 active site is not the mechanism by which PcephPT or PT inhibits  
30 NDM-1, suggesting that ternary complex formation is the likely mechanism. Spectroscopic  
31 analysis of a cobalt-substituted enzyme treated with PT and PcephPT support this ternary  
32 complex hypothesis for the mode of inhibition. Our work demonstrates that the prochelator  
33 strategy, in addition to effectively targeting antibacterial agents to drug-resistant pathogens, is a  
34  
35  
36  
37  
38  
39  
40  
41  
42  
43  
44  
45  
46  
47  
48  
49  
50  
51  
52  
53  
54  
55  
56  
57  
58  
59  
60

1  
2  
3 promising method for delivering NDM-1-inhibiting metal-binding agents in a way that improves  
4 their efficacy and provides delivery to  $\beta$ -lactamase-expressing strains.  
5  
6  
7

## 8 9 **Methods**

10  
11 **Materials.** PcephPT was synthesized as described previously.<sup>5</sup> Other compounds were  
12 purchased from commercial sources and used without further purification. Purified NDM-1  
13 enzyme was generously provided by Professor Bo Li (University of North Carolina – Chapel Hill).  
14  
15

16  
17 **Microbiology.** Preparation of *E. coli* strains expressing  $\beta$ -lactamases was described  
18 previously.<sup>5</sup> The gene sequence for NDM-1, which does not include the lipobox sequence  
19 necessary for lipidation, is provided in the Supporting Information. Antibacterial susceptibility  
20 testing was performed similarly to our previous studies. Prior to all experiments, *E. coli* carrying  
21 the appropriate plasmids was streaked onto LB agar containing 100  $\mu$ g/mL ampicillin and 50  
22  $\mu$ g/mL kanamycin. A single colony was used to inoculate 2 mL of Mueller-Hinton broth containing  
23 100  $\mu$ g/mL ampicillin and 50  $\mu$ g/mL kanamycin, which was then incubated at 37 °C, 200 rpm, for  
24 16–18 h. This overnight culture was diluted 1:500 in fresh broth and used as the working culture.  
25  
26 Compounds to be tested were serially diluted 2-fold in Mueller-Hinton broth to final concentrations  
27 ranging from 0 to 160  $\mu$ M in clear, flat-bottomed 96-well plates. The working culture, spiked with  
28 meropenem or no additional treatment was then added to the 96-well plate, giving a final inoculum  
29 dilution of 1:1000 ( $5 \times 10^5$  to  $1 \times 10^6$  CFU/mL) and final volume of 100  $\mu$ L per well. Wells containing  
30 media only were included to verify sterility. Plates were incubated for 20 h at 37 °C, 200 rpm.  
31  
32 Plates were covered with AeraSeal film (Sigma-Aldrich) during incubation to minimize  
33 evaporation.  
34  
35  
36  
37  
38  
39  
40  
41  
42  
43  
44  
45  
46  
47  
48

49  
50 Bacterial growth was evaluated by measuring the optical density at 600 nm (OD<sub>600</sub>) using  
51 a PerkinElmer Victor3 V multilabel plate reader at 0 and 20 h. The 0-h time point data were  
52 subtracted from the 20 h data to remove background medium signal. The minimum inhibitory  
53 concentration (MIC) was defined as the concentration at which no detectable growth occurred  
54  
55  
56  
57  
58

1  
2  
3 after 20 h of incubation (background subtracted  $OD_{600} < 0.010$ ). At least two biological replicates  
4 were performed with a minimum of at least four total technical replicates for each MIC  
5 determination. For timecourse growth assays, plates were incubated in the plate reader at 37 °C  
6  
7 for the duration of the assay without shaking or AeraSeal film. The initial  $OD_{600}$  for each condition  
8  
9 was subtracted from all later data points.  
10  
11  
12

13  
14 For turnover experiments in *E. coli*, an overnight culture prepared as described above,  
15 grown for 16–18 h, and diluted 1:100 in fresh Mueller-Hinton broth and incubated at 37 °C while  
16 shaking at 200 rpm for 1 h to an  $OD_{600}$  of approximately 0.04. This amount of growth was  
17 previously determined as ideal for measuring slow nitrocefin turnover over 30 min (data not  
18 shown). The culture was divided and treated with compounds for 1 h at rt. After this treatment  
19 period, each sample was lysed by sonication for 1 min and 100  $\mu$ L was immediately added to a  
20 96-well plate in triplicate wells. Nitrocefin (10  $\mu$ L) was then added quickly to each well for a final  
21 concentration of 50  $\mu$ M. The absorbance at 492 nm was measured every 5 min in a PerkinElmer  
22 Victor3 V multilabel plate reader for 30 min. Turnover rates were calculated and normalized to the  
23 untreated control.  
24  
25  
26  
27  
28  
29  
30  
31  
32  
33

34  
35 **Enzyme inhibition assays.** NDM-1 was prepared and reconstituted as described in Chan  
36 et al.<sup>27</sup> Compounds were serially diluted in 96-well plates in HEPES buffer (50 mM, pH 7.2) and  
37 incubated with NDM-1 (1 nM) for 10 min at rt. Nitrocefin (20  $\mu$ M) was added and a PerkinElmer  
38 Victor3 V multilabel plate reader was used to monitor the absorbance at 492 nm over 30 min at  
39 37 °C. The slope of the absorbance increase was normalized to that of the condition containing  
40 the least compound to determine relative NDM-1 activity. This activity was plotted against  
41  $\log(\text{concentration})$  of the compounds and GraphPad Prism software was used to calculate  $IC_{50}$   
42 values and confidence intervals. For analysis of kinetic parameters, PT and PcephPT (0–60  $\mu$ M)  
43 were incubated with 10 nM NDM-1 for 10 min at room temperature before addition of nitrocefin  
44 (63–500  $\mu$ M). The slope of the absorbance increase (492 nm) at rt was converted to normalized  
45 velocity; only linear portions of the absorbance plots were used in calculating velocities. GraphPad  
46  
47  
48  
49  
50  
51  
52  
53  
54  
55  
56  
57  
58  
59  
60

1  
2  
3 Prism software was used to fit the activity curves to the Michaelis-Menten model. The average  
4  
5  $V_{\max}$  for our kinetic experiments was 4.26  $\mu\text{M}/\text{min}$  nitrocefin for uninhibited 10 nM NDM-1.  
6

7       **Equilibrium dialysis and zinc quantification.** The following procedure was modified  
8  
9 from previous reports.<sup>34, 37, 38</sup> NDM-1 (10  $\mu\text{M}$  in a 300- $\mu\text{L}$  sample volume) was incubated in HEPES  
10  
11 (50 mM, pH 7.2) with either 4 or 16 equivalents of each compound or no compound for 30 min at  
12  
13 rt. Samples were inserted into Thermo Fisher Slide-A-Lyzer dialysis cassettes with 0.5 mL  
14  
15 sample capacity and 10K molecular weight cutoff and dialyzed against fresh HEPES (120 mL) at  
16  
17 room temperature for 4–5 h, with buffer replaced after 2 h. Samples were removed from the  
18  
19 dialysis cassettes and protein concentration was determined by measuring the absorbance and  
20  
21 280 nm and calculated using  $\epsilon_{280} = 29,760 \text{ M}^{-1}\text{cm}^{-1}$ . The samples were diluted 6-fold in 6-M  
22  
23 aqueous guanidinium chloride containing 60  $\mu\text{M}$  4-(2-pyridylazo)resorcinol (PAR) and the  
24  
25 absorbance at 500 nm was measured, for final sample concentrations of 5 M guanidinium chloride  
26  
27 and 50  $\mu\text{M}$  PAR. This was used to calculate zinc concentration using a PAR 500-nm standard  
28  
29 curve, constructed using samples of zinc sulfate in HEPES, and multiplying by 6 to determine the  
30  
31 concentration in the undiluted sample. For the samples treated with 160  $\mu\text{M}$  EDTA, the 500-nm  
32  
33 absorbance was just slightly less than that of the 0- $\mu\text{M}$  zinc sample from the standard curve,  
34  
35 which we interpret to mean that the dialyzed sample, which is depleted of zinc, contains  
36  
37 components that are chelating a small amount of zinc present in the solution of PAR and  
38  
39 guanidinium chloride; therefore, these values were not multiplied by the dilution factor of six. Zinc  
40  
41 content of NDM-1 was calculated as the ratio of zinc concentration to NDM-1 concentration.  
42  
43  
44

45       **UV-Visible spectroscopy of CoCo-NDM-1 with inhibitors.** Apo NDM-1 was generated  
46  
47 by treating purified NDM-1 (300  $\mu\text{M}$ ) with excess EDTA in HEPES (50 mM, pH 7.2) containing 2  
48  
49 mM TCEP for 30 min on ice. EDTA and metals were removed by running the sample through a  
50  
51 Micro Bio-Spin™ P-6 gel column (Bio-Rad) equilibrated with HEPES (50 mM, pH 7.2). CoCo-  
52  
53 NDM-1 was produced by adding two equivalents of  $\text{CoCl}_2$ , producing a pink sample with an  
54  
55 absorbance spectrum that is identical to previously published CoCo-NDM-1 spectra.<sup>39</sup>  
56  
57  
58

1  
2  
3 Compounds were added from 10 mM stocks in DMSO (PT, PcephPT) or water (EDTA). These  
4 volumes of DMSO were confirmed not to have any effect on the absorbance spectrum. The  
5 absorbance spectrum was collected immediately after addition of each compound and again after  
6  
7 5 and 10 min, but no changes were observed after the initial scan.  
8  
9  
10

### 11 12 13 **Supporting Information**

14  
15 The Supporting Information is available free of charge on the ACS Publications website at DOI:  
16  
17 Enzyme inhibition curves used to generate IC<sub>50</sub> values; Enzyme inhibition curves for PT and  
18 PcephPT with various incubation times; Growth of *E. coli* treated with PT and PcephPT with  
19 supplemental copper; UV-Visible absorbance spectra of apo NDM-1 and expansions of  
20 CoCoNDM-1 spectra; Kinetics of NDM-1 in the presence of PT or PcephPT; NDM-1 gene  
21 sequence expressed in *E. coli* MG1655 and UTI89 strains (PDF)  
22  
23  
24  
25  
26  
27  
28  
29

### 30 31 **Author Information**

32 Corresponding Author

33  
34 \*Phone: (919) 660-1541. Email: katherine.franz@duke.edu

35  
36 ORCID

37  
38 Abigail C. Jackson: 0000-0002-2113-3449

39  
40 Katherine J. Franz: 0000-0002-9015-0998  
41  
42  
43  
44

### 45 **Author contributions**

46  
47 K.J.F. and A.C.J. designed the research. A.C.J., J.M.Z.-B., and E.A.P performed experiments.

48  
49 K.J.F. and A.C.J. wrote the paper.  
50  
51  
52  
53

### 54 **Notes**

55  
56 The authors declare no competing financial interest.  
57  
58  
59  
60

## Acknowledgments

This project was supported in part with funds from Duke University and the National Institutes of Health (GM084176). A.C.J. acknowledges an NSF Graduate Research Fellowship (DGE 1644868). J.M.Z.-B. acknowledges fellowship support from the Duke Pharmacological Sciences Training Program (T32 GM007105). E.A.P acknowledges a Dean's Summer Research Fellowship from Duke University. We thank Professor Bo Li and Dr. Andrew N. Chan (UNC - Chapel Hill) for generously providing purified NDM-1 enzyme, Bradford Becken III (Duke University) for transforming *E. coli* strains, and Vignesh Dhanasekaran for writing scripts to expedite data analysis.

## References

1. Fisher, J. F., Meroueh, S. O., and Mobashery, S. (2005) Bacterial Resistance to  $\beta$ -Lactam Antibiotics: Compelling Opportunism, Compelling Opportunity, *Chem. Rev.* *105*, 395-424, DOI: 10.1021/cr030102i.
2. Crowder, M. W., Spencer, J., and Vila, A. J. (2006) Metallo- $\beta$ -lactamases: Novel Weaponry for Antibiotic Resistance in Bacteria, *Acc. Chem. Res.* *39*, 721-728, DOI: 10.1021/ar0400241.
3. Palzkill, T. (2013) Metallo- $\beta$ -lactamase structure and function, *Ann. N.Y. Acad. Sci.* *1277*, 91-104, DOI: 10.1111/j.1749-6632.2012.06796.x.
4. Nordmann, P., Poirel, L., Walsh, T. R., and Livermore, D. M. (2011) The emerging NDM carbapenemases, *Trends Microbiol.* *19*, 588-595, DOI: 10.1016/j.tim.2011.09.005.
5. Zaengle-Barone, J. M., Jackson, A. C., Besse, D. M., Becken, B., Arshad, M., Seed, P. C., and Franz, K. J. (2018) Copper Influences the Antibacterial Outcomes of a  $\beta$ -Lactamase-Activated Prochelator against Drug-Resistant Bacteria, *ACS Infect Dis* *4*, 1019-1029, DOI: 10.1021/acsinfecdis.8b00037.

- 1  
2  
3 6. O'Callaghan, C. H., Sykes, R. B., and Staniforth, S. E. (1976) A New Cephalosporin with a Dual  
4 Mode of Action, *Antimicrob. Agents Chemother.* **10**, 245-248, DOI:  
5 10.1128/AAC.10.2.245.  
6  
7
- 8 7. Smyth, T. P., O'Donnell, M. E., O'Connor, M. J., and St Ledger, J. O. (2000)  $\beta$ -Lactamase-  
9 Dependent Prodrugs—Recent Developments, *Tetrahedron* **56**, 5699-5707, DOI:  
10 10.1016/S0040-4020(00)00419-1.  
11  
12
- 13 8. Ma, Z., and Lynch, A. S. (2016) Development of a Dual-Acting Antibacterial Agent (TNP-2092)  
14 for the Treatment of Persistent Bacterial Infections, *J. Med. Chem.* **59**, 6645-6657, DOI:  
15 10.1021/acs.jmedchem.6b00485.  
16  
17
- 18 9. Majewski, M. W., Miller, P. A., Oliver, A. G., and Miller, M. J. (2016) Alternate “Drug” Delivery  
19 Utilizing  $\beta$ -Lactam Cores: Syntheses and Biological Evaluation of  $\beta$ -Lactams Bearing  
20 Isocyanate Precursors, *J. Org. Chem.* **82**, 737-744, DOI: 10.1021/acs.joc.6b02272.  
21  
22
- 23 10. Phelan, R. M., Ostermeier, M., and Townsend, C. A. (2009) Design and synthesis of a  $\beta$ -  
24 lactamase activated 5-fluorouracil prodrug, *Bioorg. Med. Chem. Lett.* **19**, 1261-1263, DOI:  
25 10.1016/j.bmcl.2008.12.057.  
26  
27
- 28 11. Xie, H., Mire, J., Kong, Y., Chang, M., Hassounah, H. A., Thornton, C. N., Sacchettini, J. C.,  
29 Cirillo, J. D., and Rao, J. (2012) Rapid point-of-care detection of the tuberculosis pathogen  
30 using a BlaC-specific fluorogenic probe, *Nat. Chem.* **4**, 802-809, DOI:  
31 10.1038/nchem.1435.  
32  
33
- 34 12. Liu, R., Miller, P. A., Vakulenko, S. B., Stewart, N. K., Boggess, W. C., and Miller, M. J. (2018)  
35 A Synthetic Dual Drug Sideromycin Induces Gram-Negative Bacteria To Commit Suicide  
36 with a Gram-Positive Antibiotic, *J. Med. Chem.* **61**, 3845-3854, DOI:  
37 10.1021/acs.jmedchem.8b00218.  
38  
39
- 40 13. Reeder, N. L., Kaplan, J., Xu, J., Youngquist, R. S., Wallace, J., Hu, P., Juhlin, K. D., Schwartz,  
41 J. R., Grant, R. A., Fieno, A., Nemeth, S., Reichling, T., Tiesman, J. P., Mills, T., Steinke,  
42 M., Wang, S. L., and Saunders, C. W. (2011) Zinc Pyrithione Inhibits Yeast Growth through  
43 Copper Influx and Inactivation of Iron-Sulfur Proteins, *Antimicrob. Agents Chemother.* **55**,  
44 5753-5760, DOI: 10.1128/aac.00724-11.  
45  
46
- 47 14. Reeder, N. L., Xu, J., Youngquist, R. S., Schwartz, J. R., Rust, R. C., and Saunders, C. W.  
48 (2011) The antifungal mechanism of action of zinc pyrithione, *Br. J. Dermatol.* **165 Suppl**  
49 **2**, 9-12, DOI: 10.1111/j.1365-2133.2011.10571.x.  
50  
51
- 52 15. Yasokawa, D., Murata, S., Iwahashi, Y., Kitagawa, E., Kishi, K., Okumura, Y., and Iwahashi,  
53 H. (2010) DNA microarray analysis suggests that zinc pyrithione causes iron starvation to  
54  
55  
56  
57  
58

- 1  
2  
3 the yeast *Saccharomyces cerevisiae*, *J. Biosci. Bioeng.* 109, 479-486, DOI:  
4 10.1016/j.jbiosc.2009.10.025.  
5  
6  
7 16. Park, M., Cho, Y.-J., Lee, Y. W., and Jung, W. H. (2018) Understanding the Mechanism of  
8 Action of the Anti-Dandruff Agent Zinc Pyrithione against *Malassezia restricta*, *Sci. Rep.*  
9 8, 12086, DOI: 10.1038/s41598-018-30588-2.  
10  
11  
12 17. Becker, K. W., and Skaar, E. P. (2014) Metal limitation and toxicity at the interface between  
13 host and pathogen, *FEMS Microbiol. Rev.* 38, 1235-1249, DOI: 10.1111/1574-  
14 6976.12087.  
15  
16  
17 18. Djoko, K. Y., Ong, C.-I. Y., Walker, M. J., and McEwan, A. G. (2015) The Role of Copper and  
18 Zinc Toxicity in Innate Immune Defense against Bacterial Pathogens, *J. Biol. Chem.* 290,  
19 18954-18961, DOI: 10.1074/jbc.R115.647099.  
20  
21  
22 19. Hodgkinson, V., and Petris, M. J. (2012) Copper Homeostasis at the Host-Pathogen Interface,  
23 *J. Biol. Chem.* 287, 13549-13555, DOI: 10.1074/jbc.R111.316406.  
24  
25  
26 20. Lopez Quezada, L., Li, K., McDonald, S. L., Nguyen, Q., Perkowski, A. J., Pharr, C. W., Gold,  
27 B., Roberts, J., McAulay, K., Saito, K., Somersan Karakaya, S., Javidnia, P. E., Porrás de  
28 Francisco, E., Amieva, M. M., Díaz, S. P., Mendoza Losana, A., Zimmerman, M., Liang,  
29 H.-P. H., Zhang, J., Dartois, V., Sans, S., Lagrange, S., Goullieux, L., Roubert, C., Nathan,  
30 C., and Aubé, J. (2019) Dual-Pharmacophore Pyrithione-Containing Cephalosporins Kill  
31 Both Replicating and Nonreplicating Mycobacterium tuberculosis, *ACS Infectious*  
32 *Diseases* 5, 1433-1445, DOI: 10.1021/acsinfecdis.9b00112.  
33  
34  
35 21. Ju, L.-C., Cheng, Z., Fast, W., Bonomo, R. A., and Crowder, M. W. (2018) The Continuing  
36 Challenge of Metallo- $\beta$ -Lactamase Inhibition: Mechanism Matters, *Trends Pharmacol. Sci.*  
37 39, 635-647, DOI: 10.1016/j.tips.2018.03.007.  
38  
39  
40 22. Adamek, R. N., Credille, C. V., Dick, B. L., and Cohen, S. M. (2018) Isosteres of  
41 hydroxypyridinethione as drug-like pharmacophores for metalloenzyme inhibition, *JBIC*  
42 *Journal of Biological Inorganic Chemistry* 23, 1129-1138, DOI: 10.1007/s00775-018-1593-  
43 1.  
44  
45  
46 23. Djoko, K. Y., Achard, M. E. S., Phan, M.-D., Lo, A. W., Miraula, M., Prombhul, S., Hancock,  
47 S. J., Peters, K. M., Sidjabat, H., Harris, P. N., Mitić, N., Walsh, T. R., Anderson, G. J.,  
48 Shafer, W. M., Paterson, D. L., Schenk, G., McEwan, A. G., and Schembri, M. A. (2017)  
49 Copper ions and coordination complexes as novel carbapenem adjuvants, *Antimicrob.*  
50 *Agents Chemother.* 62, DOI: 10.1128/aac.02280-17.  
51  
52  
53 24. Sun, Z., Hu, L., Sankaran, B., Prasad, B. V. V., and Palzkill, T. (2018) Differential active site  
54 requirements for NDM-1  $\beta$ -lactamase hydrolysis of carbapenem versus penicillin and  
55  
56  
57  
58  
59  
60

- 1  
2  
3 cephalosporin antibiotics, *Nature Communications* 9, 4524, DOI: 10.1038/s41467-018-  
4 06839-1.  
5  
6  
7  
8 25. Yong, D., Toleman, M. A., Giske, C. G., Cho, H. S., Sundman, K., Lee, K., and Walsh, T. R.  
9 (2009) Characterization of a New Metallo- $\beta$ -Lactamase Gene, bla<sub>NDM-1</sub>, and a Novel  
10 Erythromycin Esterase Gene Carried on a Unique Genetic Structure in *Klebsiella*  
11 *pneumoniae* Sequence Type 14 from India, *Antimicrob. Agents Chemother.* 53, 5046-  
12 5054, DOI: 10.1128/aac.00774-09.  
13  
14  
15 26. Walsh, T. R., Weeks, J., Livermore, D. M., and Toleman, M. A. (2011) Dissemination of NDM-1  
16 positive bacteria in the New Delhi environment and its implications for human health: an  
17 environmental point prevalence study, *Lancet Infect. Dis.* 11, 355-362, DOI:  
18 10.1016/S1473-3099(11)70059-7.  
19  
20  
21 27. Chan, A. N., Shiver, A. L., Wever, W. J., Razvi, S. Z. A., Traxler, M. F., and Li, B. (2017) Role  
22 for dithiolopyrrolones in disrupting bacterial metal homeostasis, *Proc. Natl. Acad. Sci. USA*  
23 114, 2717-2722, DOI: 10.1073/pnas.1612810114.  
24  
25  
26 28. Torelli, N. J., Akhtar, A., DeFrees, K., Jaishankar, P., Pemberton, O. A., Zhang, X., Johnson,  
27 C., Renslo, A. R., and Chen, Y. (2019) Active-site druggability of carbapenemases and  
28 broad-spectrum inhibitor discovery, *ACS Infectious Diseases* 5, 1013-1021, DOI:  
29 10.1021/acsinfecdis.9b00052.  
30  
31  
32 29. Krajnc, A., Brem, J., Hinchliffe, P., Calvopiña, K., Panduwawala, T. D., Lang, P. A., Kamps,  
33 J. J. A. G., Tyrrell, J. M., Widlake, E., Saward, B. G., Walsh, T. R., Spencer, J., and  
34 Schofield, C. J. (2019) Bicyclic Boronate VNRX-5133 Inhibits Metallo- and Serine- $\beta$ -  
35 Lactamases, *J. Med. Chem.* 62, 8544-8556, DOI: 10.1021/acs.jmedchem.9b00911.  
36  
37  
38 30. Meng, Z., Tang, M.-L., Yu, L., Liang, Y., Han, J., Zhang, C., Hu, F., Yu, J.-M., and Sun, X.  
39 (2019) Novel Mercapto Propionamide Derivatives with Potent New Delhi Metallo- $\beta$ -  
40 Lactamase-1 (NDM-1) Inhibitory Activity and Low Toxicity, *ACS Infectious Diseases* 5,  
41 903-916, DOI: 10.1021/acsinfecdis.8b00366.  
42  
43  
44 31. Leiris, S., Coelho, A., Castandet, J., Bayet, M., Lozano, C., Bougnon, J., Bousquet, J., Everett,  
45 M. J., Lemonnier, M., Sprynski, N., Zalacain, M., Pallin, T. D., Cramp, M., Jennings, N.,  
46 Raphy, G., Jones, M. W., Pattipati, R., Shankar, B., Sivasubrahmanyam, R., Soodhagani,  
47 A. K., Juventhala, R. R., Pottabathini, N., Pothukanuri, S., Benvenuti, M., Pozzi, C.,  
48 Mangani, S., De Luca, F., Cerboni, G., Docquier, J.-D., and Davies, D. (2018) SAR studies  
49 leading to the identification of a novel series of metallo- $\beta$ -lactamase inhibitors for the  
50 treatment of carbapenem-resistant Enterobacteriaceae infections that display efficacy in  
51 an animal infection model, *ACS Infectious Diseases* 5, 131-140, DOI:  
52 10.1021/acsinfecdis.8b00246.  
53  
54  
55  
56  
57  
58  
59  
60

- 1  
2  
3 32. Schnaars, C., Kildahl-Andersen, G., Prandina, A., Popal, R., Radix, S. L., Le Borgne, M.,  
4 Gjoen, T., Andresen, A. M. S., Heikal, A., Økstad, O. A., Fröhlich, C., Samuelsen, Ø.,  
5 Lauksund, S., Jordheim, L. P., Rongved, P., and Åstrand, O. A. H. (2018) Synthesis and  
6 preclinical evaluation of TPA-based zinc chelators as metallo- $\beta$ -lactamase inhibitors, *ACS*  
7 *Infectious Diseases* 4, 1407-1422, DOI: 10.1021/acsinfecdis.8b00137.  
8  
9  
10 33. Everett, M., Sprynski, N., Coelho, A., Castandet, J., Bayet, M., Bougnon, J., Lozano, C.,  
11 Davies, D. T., Leiris, S., Zalacain, M., Morrissey, I., Magnet, S., Holden, K., Warn, P., De  
12 Luca, F., Docquier, J.-D., and Lemonnier, M. (2018) Discovery of a Novel Metallo- $\beta$ -  
13 Lactamase Inhibitor That Potentiates Meropenem Activity against Carbapenem-Resistant  
14 Enterobacteriaceae, *Antimicrob. Agents Chemother.* 62, DOI: 10.1128/aac.00074-18.  
15  
16  
17 34. Chen, A. Y., Thomas, P. W., Stewart, A. C., Bergstrom, A., Cheng, Z., Miller, C., Bethel, C.  
18 R., Marshall, S. H., Credille, C. V., Riley, C. L., Page, R. C., Bonomo, R. A., Crowder, M.  
19 W., Tierney, D. L., Fast, W., and Cohen, S. M. (2017) Dipicolinic Acid Derivatives as  
20 Inhibitors of New Delhi Metallo- $\beta$ -lactamase-1, *J. Med. Chem.* 60, 7267-7283, DOI:  
21 10.1021/acs.jmedchem.7b00407.  
22  
23  
24 35. Pankey, G. A., and Sabath, L. D. (2004) Clinical Relevance of Bacteriostatic versus  
25 Bactericidal Mechanisms of Action in the Treatment of Gram-Positive Bacterial Infections,  
26 *Clin. Infect. Dis.* 38, 864-870, DOI: 10.1086/381972.  
27  
28  
29 36. Bahr, G., Vitor-Horen, L., Bethel, C. R., Bonomo, R. A., González, L. J., and Vila, A. J. (2018)  
30 Clinical Evolution of New Delhi Metallo- $\beta$ -Lactamase (NDM) Optimizes Resistance under  
31 Zn(II) Deprivation, *Antimicrob. Agents Chemother.* 62, DOI: 10.1128/aac.01849-17.  
32  
33  
34 37. Thomas, P. W., Zheng, M., Wu, S., Guo, H., Liu, D., Xu, D., and Fast, W. (2011)  
35 Characterization of Purified New Delhi Metallo- $\beta$ -lactamase-1, *Biochemistry* 50, 10102-  
36 10113, DOI: 10.1021/bi201449r.  
37  
38  
39 38. Chen, A. Y., Thomas, P. W., Cheng, Z., Xu, N. Y., Tierney, D. L., Crowder, M. W., Fast, W.,  
40 and Cohen, S. M. (2019) Investigation of Dipicolinic Acid Isosteres for the Inhibition of  
41 Metallo-beta-Lactamases, *ChemMedChem* 14, 1271-1282, DOI:  
42 10.1002/cmdc.201900172.  
43  
44  
45 39. Yang, H., Aitha, M., Marts, A. R., Hetrick, A., Bennett, B., Crowder, M. W., and Tierney, D. L.  
46 (2014) Spectroscopic and Mechanistic Studies of Heterodimetallic Forms of Metallo- $\beta$ -  
47 lactamase NDM-1, *J. Am. Chem. Soc.* 136, 7273-7285, DOI: 10.1021/ja410376s.  
48  
49  
50 40. Bergstrom, A., Katko, A., Adkins, Z., Hill, J., Cheng, Z., Burnett, M., Yang, H., Aitha, M.,  
51 Mehaffey, M. R., Brodbelt, J. S., Tehrani, K. H. M. E., Martin, N. I., Bonomo, R. A., Page,  
52 R. C., Tierney, D. L., Fast, W., Wright, G. D., and Crowder, M. W. (2017) Probing the  
53 Interaction of Aspergillomarasmine A with Metallo- $\beta$ -lactamases NDM-1, VIM-2, and IMP-  
54 7, *ACS Infectious Diseases* 4, 135-145, DOI: 10.1021/acsinfecdis.7b00106.  
55  
56  
57  
58  
59  
60

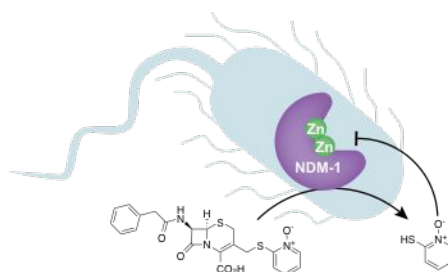
1  
2  
3  
4  
5  
6  
7  
8  
9  
10  
11  
12  
13  
14  
15  
16  
17  
18  
19  
20  
21  
22  
23  
24  
25  
26  
27  
28  
29  
30  
31  
32  
33  
34  
35  
36  
37  
38  
39  
40  
41  
42  
43  
44  
45  
46  
47  
48  
49  
50  
51  
52  
53  
54  
55  
56  
57  
58  
59  
60

## For Table of Contents Only

**A Cephalosporin Prochelator Inhibits New Delhi Metallo- $\beta$ -Lactamase 1 without Removing Zinc**

Abigail C. Jackson, Jacqueline M. Zaengle-Barone, Elena A. Puccio, Katherine J. Franz\*

Department of Chemistry, Duke University, 124 Science Drive, Durham, North Carolina 27708, United States



PcephPT, an antibacterial pro-chelator that releases the metal-binding agent pyridine (PT) upon cleavage by  $\beta$ -lactamases, inhibits the metallo- $\beta$ -lactamase NDM-1. PcephPT restores the activity of a carbapenem antibiotic against NDM-1-expressing *E. coli* and presents a promising strategy for development of targeted metallo- $\beta$ -lactamase inhibitors.